Binary Oscillatory Crossflow Electrophoresis

Richard F. Molloy, Christopher T. Gallagher, and David T. Leighton, Jr.
Department of Chemical Engineering, University of Notre Dame

1 Summary

Electrophoresis has long been recognized as an effective analytic technique for the separation of proteins and other charged species, however attempts at scaling up to accomodate commercial volumes have met with limited success. In this report we describe a novel electrophoretic separation technique - Binary Oscillatory Crossflow Electrophoresis (BOCE). Numerical simulations indicate that the technique has the potential for preparative scale throughputs with high resolution, while simultaneously avoiding many problems common to conventional electrophoresis. The technique utilizes the interaction of an oscillatory electric field and a transverse oscillatory shear flow to create an active binary filter for the separation of charged protein species. An oscillatory electric field is applied across the narrow gap of a rectangular channel inducing a periodic motion of charged protein species. The amplitude of this motion depends on the dimensionless electrophoretic mobility, $\alpha = \frac{E_o \mu}{\omega d}$, where E_o is the amplitude of the electric field oscillations, μ is the dimensional mobility, ω is the angular frequency of oscillation and d is the channel gap width. An oscillatory shear flow is induced along the length of the channel resulting in the separation of species with different mobilities. We present a model that predicts the oscillatory behavior of charged species and allows estimation of both the magnitude of the induced convective velocity and the effective diffusivity as a function of α in infinitely long channels. Numerical results indicate that in addition to the mobility dependence, the steady state behavior of solute species may be strongly affected by oscillating fluid into and out of the active electric field region at the ends of the cell. The effect is most pronounced using time dependent shear flows of the same frequency ($\cos(\omega t)$ flow mode) as the electric field oscillations. Under such conditions, experiments indicate that solute is drawn into the cell from reservoirs at both ends of the cell leading to a large mass build up. As a consequence, any initially induced mass flux will vanish after short times. This effect was not captured by the infinite channel model and hence numerical and experimental results deviated significantly. The revised model including finite cell lengths and reservoir volumes allowed quantitative predictions of the time history of the concentration profile throughout the system. This latter model accurately describes the fluxes observed for both oscillatory flow modes in experiments using single protein species. Based on the results obtained from research funded under NASA grant NAG-8-1080.S, we conclude that binary separations are not possible using purely oscillatory flow modes because of end effects associated with the $\cos(\omega t)$ mode. Our research shows, however, that a combination of $\cos(2\omega t)$ and steady flow should lead to efficient separation free of end effects. This possibility is currently under investigation.

2 Students supported:

There were two under NASA grant NAG-8-1080.S over the award period 8/94 - 2/97:

1)Richard Molloy, Ph.D. exp. (1998), "Binary Oscillatory Crossflow Electrophoresis"

2)Yolanda Van Lishout, Ph.D. (1997), "Oscillatory Membrane Separations"

A portion of the latter thesis work dealt with dispersion produced from oscillatory flows in parallel channels. This research provided valuable insight into dispersion observed in the BOCE

cell and suggested possible geometries for scaleup of an electrophoretic device.

3 Publications:

Publications resulting from this grant include:

1)Molloy, Richard F., Christopher T. Gallagher, and David T. Leighton, Jr., "Binary Oscillatory Crossflow Electrophoresis," NASA Conference Publication. n 3338 1996. NASA, Cleveland, OH, USA p 723-728

2)In addition, two manuscripts detailing work supported in part by this grant are being prepared for publication.

3)The results of this work will be presented at the annual AIChE conference in Los Angeles, CA in 11/97.

Binary Oscillatory Crossflow Electrophoresis: Applications to Large Scale Separations

Summary of Research

NASA grant: NAG-8-1080.S

period covered by report: 8/94 - 2/97

Dr. David T. Leighton, Jr.

182 Fitzpatrick Hall
Department of Chemical Engineering
University of Notre Dame
(219) 631-5580

May 30, 1997

Contents

1 Introduction. 1

2 Background. 1
- 2.1 Conventional Electrophoresis Techniques. 2
- 2.2 Field Flow Fractionation Techniques. 2
- 2.3 Novel methods. 3

3 Theory. 5
- 3.1 Analytical Model. 5
- 3.2 Analytical Results. 5
- 3.3 Numerical Results for an Infinite Channel. 7
- 3.4 Characteristic Performance. 9

4 Experimental. 10
- 4.1 Experimental Setup. 10
- 4.2 Results. 11

5 Numerical Results including Channel End Regions. 17

6 Conclusions 20

7 References 21

8 Students supported under this grant 23

9 Publications resulting from this grant 23

1 Introduction.

The separation and purification of biochemicals is vital to many industries. For example, whey proteins and other macromolecules are concentrated from cheeses and used to fortify certain milk products in the dairy industry. Additionally, many biochemicals represent active ingredients in drugs and medicines produced as pharmaceuticals. Techniques for producing pure proteins, for example, such as density centrifugation and crystallization, although capable of large throughputs, are particularly harsh on solute species and can result in denaturation. In 1937, Tisilius [1] demonstrated experimentally that electrophoresis could be used to isolate very similar blood proteins under much milder processing conditions, i.e. separations could be conducted in actual biological mediums preventing the potentially damaging effects of denaturation. Since this discovery, the technique has received widespread attention and various versions of the original approach have emerged, all with the intent of increasing both throughput and resolution. While high resolution has been achieved on a lab scale, scaleup has experienced limited success. Consequently, electrophoresis has remained a primarily analytical technique.

Recently, our research group has developed a novel approach to electrophoretic separations, Binary Oscillatory Crossflow Electrophoresis (BOCE). The technique uses the interaction of an oscillatory electric field and a transverse oscillatory shear flow to create an active binary filter for the segregation of charged species. An oscillatory electric field is applied across the narrow gap of a rectangular channel inducing a periodic motion of charged protein species. The amplitude of this motion depends on the dimensionless electrophoretic mobility, $\alpha = \frac{E_o \mu}{\omega d}$, where E_o is the amplitude of the electric field oscillations, μ is the dimensional mobility, ω is the angular frequency of oscillation and d is the channel gap width. An oscillatory shear flow is induced along the length of the channel resulting in the separation of species with different mobilities. Preliminary results indicate that the technique may achieve larger throughputs than conventional electrophoretic methods while retaining the high resolution achieved on a laboratory scale. The primary goal of the research conducted under NASA grant NAG-8-1090.S was to develop the BOCE technique for large scale protein separations.

2 Background.

Electrophoresis describes the motion of charged particles or molecules relative to the bulk fluid under an external electric field. Smoluchowski(1903) and Huckel(1924) [2] showed that the velocity of a charged species was proportional to the electric field strength and the electrophoretic mobility, μ. The mobility was defined as the velocity per unit field strength, and was determined to be related to the size and charge of the particle as well as properties of the surrounding fluid. Tisilius later used the information to experimentally demonstrate the utility of electrophoresis for protein separations [1] in 1937. Since that time, the technique has been widely acknowledged as an attractive method for both analytical and preparative biochemical separations due mainly to the mild processing conditions. A review of the history and progress of modern electrophoresis is given by Ivory [4].

2.1 Conventional Electrophoresis Techniques.

One attractive form of electrophoresis is thin-film continuous free-flow electrophoresis (CFFE). In a typical continuous free-flow device, mixed solute is fed into a stream of carrier electrolyte flowing through a thin 0.5 to 1.0 mm gap between two electrodes that bound the gap width, and an electric field applied transverse to the carrier flow separates the solute into zones. The distance each molecule moves between the electrodes is proportional to the magnitude of the electric field and the species electrophoretic mobility, which is $O(10^{-6}\frac{cm\mu m}{Vsec})$. The small solute velocities require carrier flow rates and channel lengths such that experimental times are approximately one hour [4] and, consequently, throughputs are usually limited to a few milligrams of purified solute in that time span.

The throughput in a CFFE device may be increased by increasing the electric field strength (which increases the solute velocities), however power dissipation, or Joule heat, in the fluid is proportional to ${E_o}^2\sigma$, where E_o is the electric field magnitude and σ is the conductivity of the carrier fluid. The heat may be removed by wall cooling, however temperature gradients in the fluid may lead to buoyancy driven instabilites. Viscous stabilization can be increased with smaller gap thicknesses, however this further diminishes the throughput. Even if buoyancy driven instabilites are eliminated, crescent dispersion, electroosmosis [4] and electrohydrodynamic mixing [5], [6] may limit the resolution of the CFFE system.

If the electric field is applied across the narrow dimension of the gap, the effects of crescent dispersion and electroosmosis can be reduced. However this configuration requires larger electric fields to separate solute because the distance species must migrate before exiting the device is significantly decreased. Consequently, the increased electric fields may destabilize the system. Philpot [8] overcame these difficulties and created one of the more successful high throughput CFFE devices. His device uses an electric field across the annular gap of a rotating Couette device with the channel aligned vertically. The centrifugal forces and the vertical alignment stabilize the effects of large electric fields and, consequently, buoyancy driven mixing is reduced. A commercially available separator based on this design is capable of processing about $10g$ of protein per hour, however difficulties involved with extracting the narrow bands of solute from the device limit the resolution.

2.2 Field Flow Fractionation Techniques.

Another approach similar to electrophoresis is Electrical Field Flow Fractionation (EFFF) [7]. This technique combines laminar flow of carrier electrolyte in a channel with a transverse electric field to separate components of a complex mixture. As the field is applied, protein species are focused into regions near the wall. The distance these zones extend away from the wall is due to an equillibrium balance between the focusing effect of the electric field and diffusion, hence elution of a species from the device is inversely proportional to the species' electrophoretic mobility. While this technique experimentally agrees with theory at low electric field strengths, the resolution is poor. The large electric fields required for a sharp separation were found to effectively immobilize proteins in the device [3]. Attempts have been made to improve this technique by experimenting with different channel geometries [9], or by introducing transverse pH gradients [10], however little progress has been

made. Consequently, EFFF remains a small scale batch elution technique.

In order to improve the throughput of EFFF, Giddings [11] proposed a method to eliminate the immobilization of species at high values of the applied field. This technique, termed Cyclical Electric Field Flow Fractionation, or CEFFF, uses a cyclical electric field to induce periodic motion of solute. The induced solute motion when coupled with a steady flow leads to a time averaged solute velocity through the cell that is a function of the mobility. Because the migration across the gap is not limited by the ratio of the molecular diffusivity to the electrophoretic mobility, larger electric fields and hence throughputs are potentially achievable.

2.3 Novel methods.

Shmidt and Cheh proposed a new technique similar to CEFFF applicable to continuous separations[12]. In addition to a steady flow and a transverse periodic electric field, Shmidt and Cheh proposed a third direction of motion - a periodic pulsating flow - acting perpendicuar to both the steady flow and the field. The system was modelled numerically, ignoring the effect of diffusion. Numerical results indicate that their method is capable of separating solute species whose electrophoretic mobilities differ by $0.1\frac{\mu mcm}{Vsec}$. These predictions have yet to be verified experimentally.

Chandhok and Leighton [13] recently proposed a technique similar to that of Shmidt and Cheh. In this method, an oscillatory - rather than pulsed - crossflow is coupled with an oscillatory electric field. By using an oscillatory flow it is possible to induce the migration of species with different electrophoretic mobilities in opposite directions. Chandhok and Leighton developed an analytical model for the motion of solute species in the absence of diffusion. In addition to ignoring diffusion, their solution neglects the no flux boundary conditions at the walls. This simplifies the model, however it also limits the possible operating parameters of the system. Nevertheless, they were able to show that the separation could be optimized for a given combination of oscillatory electric field and crossflow modes. Furthermore, since the solute molecules migrate to a particular streamline regardless of the initial position, then solute could be fed across the entire width of the gap. The resulting throughput represents a large increase over conventional devices that feed solute at only one point.

Although the proposed methods of Shmidt and Cheh and Chandhok and Leighton seem promising, an actual experimental device implementing either would be difficult to design because it requires precise control of simultaneous fluid flow in two directions. Our research group has recently developed a novel technique that combines the most desirable features of Chandhok and Leighton's method while avoiding the complexity of controlling fluid flow in two directions. This technique, Binary Oscillatory Crossflow Electrophoresis, is theoretically capable of separating one component from a complex mixture while having the potential for significant improvements in throughput and resolution over conventional CFFE techniques. This method relies on the interaction of an oscillatory electric field and a transverse oscillatory shear flow, shown in Figure (1). As mentioned earlier, an oscillatory electric field applied across the thin dimension of a rectangular channel induces a periodic

motion of charged protein species. The amplitude of this motion depends on the dimensionless electrophoretic mobility, $\alpha = \frac{E_o \mu}{\omega d}$, where E_o is the amplitude of the electric field, μ is the dimensional electrophoretic mobility, ω is the angular frequency of oscillation and d is the channel gap thickness. An oscillatory shear flow is induced along the length of the channel resulting in the separation of species with different mobilities. Appropriate selection of frequency and phase of oscillation of the two interacting driving forces provides an effective filter that will allow proteins either higher or lower than a chosen electrophoretic mobility to pass through the device. The technique could be used for both analytical and preparative work by programming the filter setpoint to change with time and collecting the purified species that pass through the device at each setpoint. For continuous isolation of a particular fraction from a complex mixture feed, a network of these devices could be used.

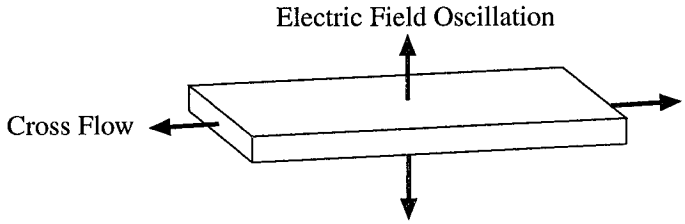

Figure 1: Direction of motions in a binary oscillatory crossflow electrophoresis cell.

In the next section, the effect of coupled oscillatory electric and flow fields on the motion of charged solute species is modelled for a thin channel geometry. The analytical solution presented is possible in the limit of zero diffusion. It will be shown that for a particular choice of oscillatory electric field, the only modes of a general Fourier series that lead to solute migration are a steady mode, $cos(\omega t)$ mode and $cos(2\omega t)$. These results closely resemble the work of Chandkok and Leighton [13]. The applicability of the model is extended using numerical simulations including diffusion for the case of an infinitely long channel, and the induced migration velocity and effective axial diffusivity are calculated as a function of the dimensionless mobility α and the dimensionless diffusivity $\lambda = \frac{D}{d^2 \omega}$ for purely oscillatory flows. Included is a comparison of the predicted performance of the BOCE system with conventional CFFE units in the infinite channel limit.

In section four, we describe the experimental system used to verify the model predictions. Single protein experiments using Bovine Serum Albumen (BSA) and Bovine Hemoglobin (BHb) were conducted and are shown to agree well with our model for one choice of oscillatory shear flow - $\bar{u} = \Delta x \omega cos(2\omega t)$, where Δx is the oscillatory tidal displacement, while large discrepancies are observed for oscillatory shear flows at half this angular frequency. Reasons for this discrepancy are discussed in section five. It will be shown that oscillating fluid into and out of the active electric field region has a large effect on the time history of the concentration profile. Using a revised numerical model including the cell end regions, quantitative agreement with experiments under both sets of flow conditions is observed. We conclude with a summary of results and conclusions.

3 Theory.

3.1 Analytical Model.

In the following analysis, we examine the effect of two oscillatory driving forces, an electric field and a shear flow, on the motion of charged solute species in the absence of diffusion. Here we have chosen the x-axis to be along the channel length and the y-axis to be across the thin gap (between the electrodes). The motion of charged species in the y-direction is a function of the electrophoretic mobility, μ, and the time dependent electric field:

$$\frac{dy}{dt} = \mu E_o h(\omega t) = \frac{\mu E_o}{\omega}\frac{d}{dt}g(\omega t) \tag{1}$$

where y is the solute position in the gap, t is the time, ω is the frequency of oscillation, E_o is the electric field strength, $h(\omega t)$ describes the oscillation of the electric field, and $g(\omega t)$ describes the oscillatory motion of the solute in the y direction. If we integrate equation (1), the time dependent solute position in the gap is given by:

$$\frac{y}{d} = \alpha g(\omega t) \tag{2}$$

Here we have defined $\alpha = \frac{\mu E_o}{\omega d}$ as the dimensionless electrophoretic mobility for gap thickness d.

The convective motion in the x direction can be written as

$$u_x = 4u_{max}\frac{y}{d}\left(1 - \frac{y}{d}\right) f(\omega t) \tag{3}$$

where u_x is the fluid velocity in the x direction, u_{max} is the velocity of the center line, and $f(\omega t)$ is the oscillatory component to the flow. If we substitute the solute position from equation (2) into equation (3) and take the time average over one period of oscillation, we have an equation describing the motion of a solute molecule in the absence of molecular diffusion:

$$\left\langle \frac{dx}{dt} \right\rangle = 4u_{max}\alpha\left(\left\langle g(\omega t)f(\omega t)\right\rangle - \alpha\left\langle g(\omega t)^2 f(\omega t)\right\rangle\right) \tag{4}$$

where $\langle\cdot\rangle$ is the time average over one period. Here we see that the velocity of a particular solute species through the channel is a function of the interaction between the two time dependent functions, $f(\omega t)$ and $g(\omega t)$, and the electrophoretic mobility, α.

3.2 Analytical Results.

With equation (4) we may evaluate the solute velocity across the channel for combinations of arbitrary choices for $f(\omega t)$ and $g(\omega t)$. Chandhok and Leighton [13] chose $g(\omega t) = 1 - \cos(\omega t)$ and showed that the only modes of a general Fourier series $f(\omega t)$ that contributed to solute migration (in the x direction) were a steady flow, $\cos(\omega t)$, and $\cos(2\omega t)$. The time averaged velocity for each of these three individual modes using the above choice of $g(\omega t)$ is given by:

$$\left\langle \frac{dx}{dt} \right\rangle \Bigg|_{steady} = 2\alpha(2 - 3\alpha)$$

$$\left\langle \frac{dx}{dt} \right\rangle \Big|_{cos(\omega t)} = 2\alpha(2\alpha - 1)$$
$$\left\langle \frac{dx}{dt} \right\rangle \Big|_{cos(2\omega t)} = -\alpha^2$$

and are shown in Figure (2) as a function of the dimensionless mobility α.

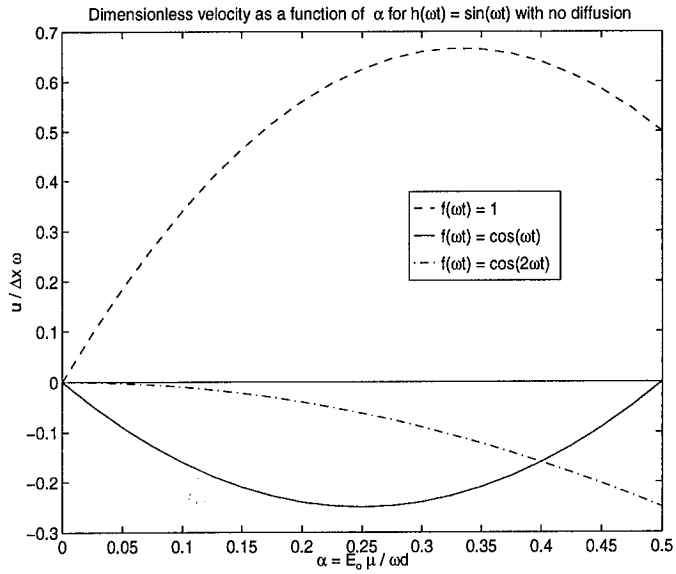

Figure 2: Plot of dimensionless velocity versus dimensionless electrophoretic mobility in the absence of cross-streamline diffusion.

Note that the steady mode leads to positive solute velocities for all values of α, while the $cos(\omega t)$ and $cos(2\omega t)$ modes lead to negative velocities. For a binary separation, the velocity must change sign at some critical value of α. Thus species with mobilities less than the critical value will be retained in the device, and those with larger mobilities will be allowed to pass, or vice versa. Although none of the choices for $f(\omega t)$ satisfy this constraint individually, the structure of our equations allows us to combine the flow modes to produce a separation. The velocity for one combination, $f(\omega t) = cos(\omega t) - cos(2\omega t)$, is shown in Figure (3). Note that in addition to satisfying the above criteria for a binary separation, $\frac{d(u/u_{max})}{d\alpha}$ through the critical mobility is large, a condition for sharp separation. A more detailed analysis concerning the optimal choice of modes for a given separation is given in [13].

Although the analytical model provides the qualitative system performance, it is limited in several ways. First, neglecting diffusion places a serious limitation on the range of applicability of the model. Aris and others [14], [15] have shown that diffusion in the direction of fluid motion can be enhanced by several orders of magnitude in the presence of steady and oscillatory shear flows. Additionally, the above analytical solution confines solute positions to $0 \leq y \leq d$. For our choice of $g(\omega t)$, this limits the dimensionless mobilities to $0.0 \leq \alpha \leq 0.5$. Consequently, optimal operating parameter ranges may be omitted.

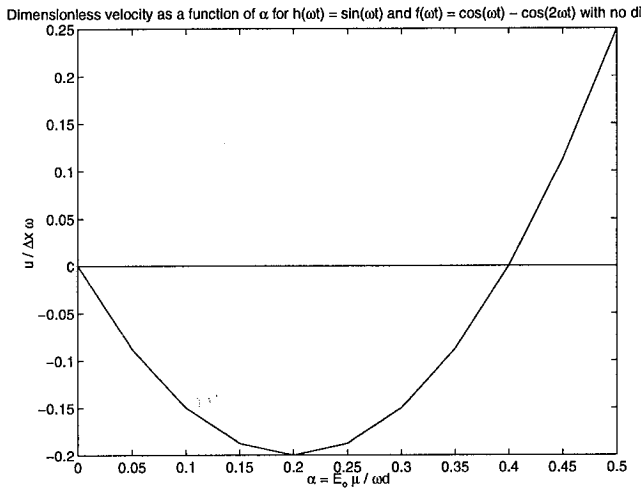

Figure 3: Plot of dimensionless velocity versus dimensionless electrophoretic mobility for a flow waveform that satisfies the criteria for a binary separation in the absence of cross-streamline diffusion.

3.3 Numerical Results for an Infinite Channel.

In order to better characterize solute motion, we performed numerical simulations using a discretized form of the Langevin equation including appropriate boundary conditions. At each time step, we added a random walk of length $\sqrt{2\lambda\Delta t}$, where $\lambda = \frac{D}{d^2\omega}$, to the electrophoretic motion of 1000 molecules and recorded the mean position and variance of the solute distribution. The data was used to determine the time averaged solute velocity and the effective diffusion coefficient in the direction of motion of the solute. We ran the simulation until the mean position and variance became linear in time.

For our simulation, we considered a protein molecule with with dimensional mobility μ and diffusivity D. We chose to fix the gap width d and the angular frequency ω and adjust the electric field amplitude to achieve desired values of α. Consequently, our choice of the above parameters fixed the dimensionless diffusivity, λ. For the flow, we chose the purely oscillatory modes $cos(\omega t)$, $\cos(2\omega t)$, and $cos(\omega t) - cos(2\omega t)$ waveforms, and for the electric field $sin(\omega t) - 0.05$. The small steady bias to the electric field was added to refocus the solute toward the lower wall at the beginning of each time period. The simulated solute velocity as a function of α and λ for $f(\omega t) = cos(\omega t) - cos(2\omega t)$ is shown in Figure (4) along with the $\lambda = 0$ result. Note that the shape of both curves is similar, however the numerical results are shifted because of the electric field bias used in the simulations. A more detailed discussion of the role of the bias is given in later sections.

The calculated dispersion produced by the combined oscillatory mode $cos(\omega t) - \cos(2\omega t)$ is depicted in figure (5). Note the increased diffusive enhancement for solute that spends longer times at short distances from the wall for $\alpha \leq 0.5$. In these regions, the competing action of electrophoretic migration, bias focusing and diffusion in the y direction approach similar magnitudes. The sudden drop around $\alpha = 0.5$ is caused by a much stronger focussing at both the upper and lower walls resulting from the unconstrained amplitude of the

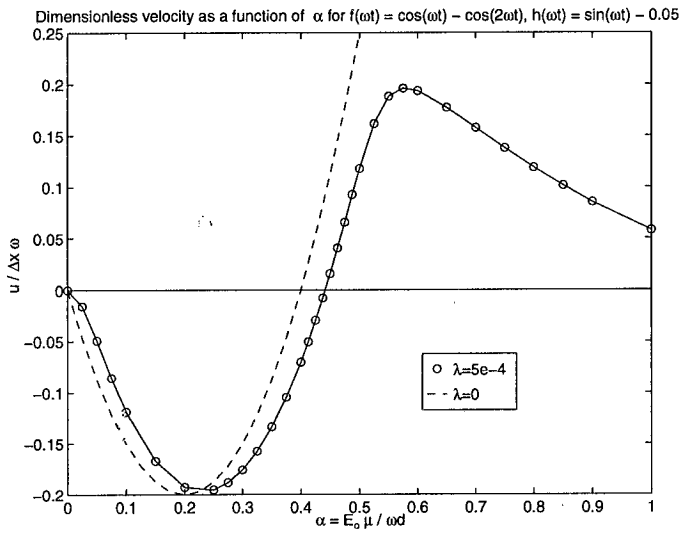

Figure 4: Plot of dimensionless velocity versus dimensionless electrophoretic mobility including the effects of cross-streamline diffusion.

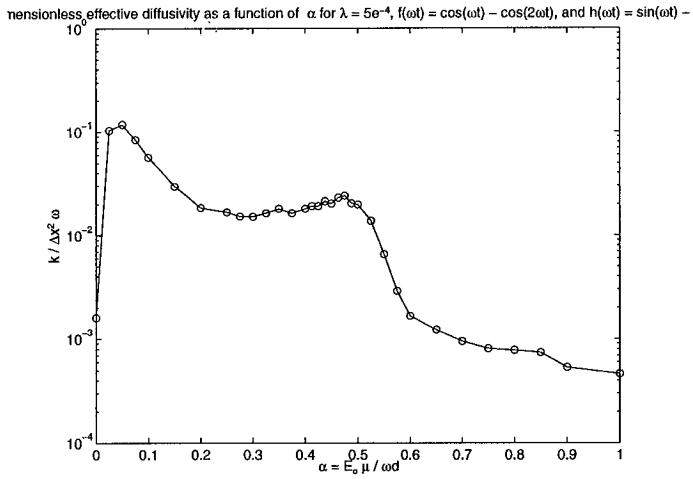

Figure 5: Plot of dimensionless effective diffusivity versus dimensionless electrophoretic mobility.

electrophoretic motion exceeding the dimension of the gap. The dispersion acts to reduce the selectivity of the binary separator.

3.4 Characteristic Performance.

To determine the characteristic throughput of our system, we performed order of magnitude calculations. Consider a cell with a separation chamber with length L, width W, and thickness d connecting two well mixed reservoirs located at $x = 0$ and $x = L$ (subscripts 1 and 2), respectively, shown in Figure (6). Let V_1 and V_2 and c_1 and c_2 represent the vol-

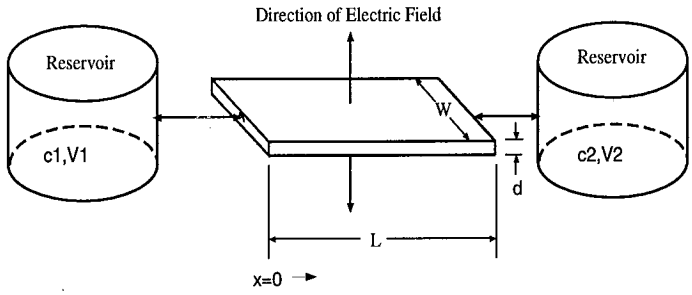

Figure 6: Diagram of a characteristic electrophoretic system.

umes and solute concentrations in the reservoirs at these locations. If the reservoir volumes are much greater than the cell volume, then the concentration profile in the cell will reach pseudo steady-state. With this approximation the dimensionless flux is thus given by:

$$N_x^*(t) = u^* \frac{c_1^*(t^*) \exp\left(\frac{u^* L^*}{k_{eff}^*}\right) - c_2^*(t^*)}{\exp\left(\frac{u^* L^*}{k_{eff}^*}\right) - 1} \tag{5}$$

where $u^* = \frac{u}{u_{max}}$, $k_{eff}^* = \frac{k_{eff}}{u_{max}^2/\omega}$, $L^* = \frac{L}{\Delta x}$, $N_x^* = \frac{N_x}{c_1(0)u_{max}}$ and $u_{max} = \Delta x \omega$ where Δx is the amplitude of fluid oscillation.

Figure (7) shows a plot of N_x^* as a function of α for an effective channel length $L^* = 2.5$, and time dependent shear flow components $f(\omega t) = cos(\omega t) - \cos(2\omega t)$ and $f(\omega t) = \cos(2\omega t) - \cos(\omega t)$. For maximum throughput, one reservoir is held at constant concentration (either c_1 or c_2) while the other is flushed with buffer to maintain a concentration of 0. Finally, values of u^* and k_{eff}^* are taken from Figures (4) and (5) for a dimensionless diffusivity $\lambda = 5e^{-4}$. Clearly the flux dramatically changes near the critical mobility at $\alpha \sim 0.45$ for both choices of $f(\omega t)$. For a 10% change in α about this point, the flux increases two orders of magnitude. Note the small peak present for low α values using the $\cos(2\omega t) - \cos(\omega t)$ waveform. This peak represents the effect of large dispersion and simultaneous low induced velocity at low values of α. Under these conditions, larger tidal displacements decrease the distance over which concentration gradients develop, leading to higher effective diffusive fluxes. To avoid the potentially damaging effects of this peak on resolution, care must be taken in choosing operating parameter ranges for high mobility separations.

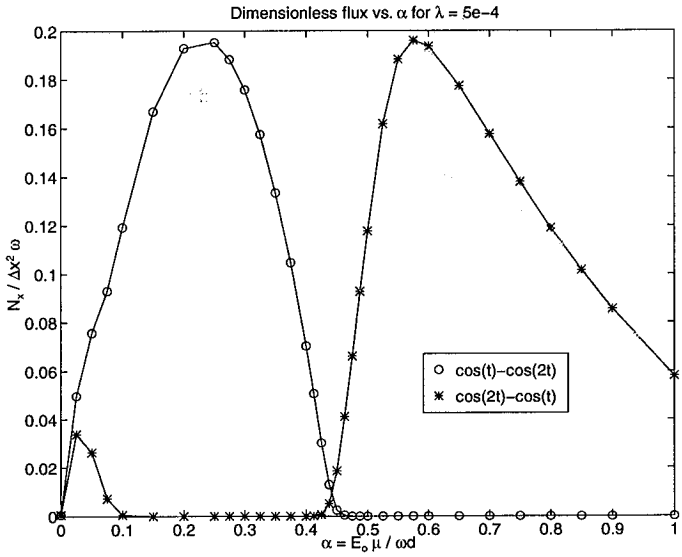

Figure 7: Plot of Dimensionless Flux versus dimensionless electrophoretic mobility.

We can compare the predicted throughput of our system with typical CFFE devices using a two protein mixture. For this case we use $1.0wt\%$ solutions of Hemoglobin (Hb) and Serum Albumin (SA) proteins with characteristic dimensional mobilities of $\mu_{Hb} = 17.4e^{-5}$ and $\mu_{SA} = 8.0e^{-5}\frac{cm^2}{Vs}$ [16]. Using $\omega = 0.136s^{-1}$, $d = 0.1cm$, and $E_o = 45V/cm$, the dimensionless mobilities are $\alpha_{Hb} = 0.575$ and $\alpha_{SA} = 0.25$. For a cell of length $L = 20.0cm$ and width $W = 6.0cm$, we calculate throughputs of $4.59g/hr$ for SA protein using $f(\omega t) = cos(\omega t) - \cos(2\omega t)$ and $4.61g/hr$ for Hb protein using $f(\omega t) = cos(2\omega t) - \cos(\omega t)$ (the second protein in each case had essentially zero flux). These throughputs represent several orders of magnitude improvement over typical CFFE devices using concentrations far below the solubility limits of these proteins[4].

4 Experimental.

4.1 Experimental Setup.

To verify the analytical and numerical results of the BOCE technique, an experimental system including a single binary separation cell, two reservoirs and an electrolyte bath was constructed. The separation cell is similar to that of Giddings [7], and allows continuous flow of solute in a buffer solution through a thin separation chamber between two membranes. The cell used in our earliest experiments contained a separation channel 20.0 *cm* long, 5 *cm* wide and 0.1 *cm* thick. Solute and buffer were fed through small syringes at the inlet and outlet of the cell. The design was eventually abandoned due to fluctuations in channel volume caused by the large pressure drops across the syringe and insufficient membrane support.

The redesigned BOCE cell is much smaller than the original version, and is being used

for all of our current work. The central separation chamber of this cell is 10 cm long, 3 cm wide, and 0.1 cm thick and was machined from a plastic sheet divided into two halves to accomodate solute feed across the entire 3.0 cm channel width. Fluid is introduced at either end of the separation chamber through plexiglass manifolds connected to the reservoirs via small polypropylene fittings and tubing. The separation chamber is sandwiched between two stretched regenerated cellulose membranes directly supported by electrode screens. The layers are clamped between two plexiglass blocks each with a central rectangular opening approximately the size of the separation chamber. The separation cell is shown in Figure (8).

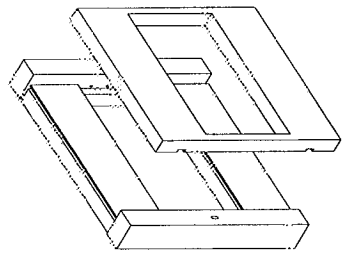

Figure 8: Diagram of the BOCE separation cell

Gas bubbles and Joule heat are removed by submerging the entire cell in an electrolyte bath open to atmosphere. The bath accommodates up to 6 liters of electrolyte fluid and copper cooling coils that control the temperature difference between the bath and the exit reservoir. The cell is positioned in the bath with the 5.0 cm side forming the vertical axis, and gas bubbles generated from electrode reaction are removed from the electrodes through the rectangular openings in the cell block halves.

The oscillatory electric fields were generated by driving constant amplitude currents in the electrolyte using a KEPCO BOP100-4M bipolar power supply controlled by LabVIEWs software. Bulk fluid conductivity and temperature data were measured with a Cole-Parmer conductivity meter. The data was simultaneously fed into LabVIEWs and the amplitude of the current waveform was adjusted to maintain a constant electric field amplitude. The flow waveforms were delivered by a specially designed syringe pump using a Galil DMC-1500 motion controller and software. Position data from the syringe pump was fed back into LabVIEW allowing phase locking of the two driving forces to within a few milliseconds. The pH was measured using an Omega PHH-3X meter accurate to +/- 0.1 units. Protein concentration was analyzed using a Varian UV-VIS spectrometer using refractive index matched cuvettes allowing 80% transmission at $200nm$. Absorbance intensities were measured in the range of 0.1 to 1.0 cm^{-1} with accuracy of +/- 0.002 cm^{-1}.

4.2 Results.

The focus of our preliminary experiments was to test the predictions of our model in two ways. First, we sought to examine the phase dependence of the flux on our waveforms. In

addition to checking our model, we would be demonstrating the utility of the technique for both high and low mobility separations. Next, we sought to demonstrate that changing the dimensionless mobility, α, by changing either the amplitude of the electric field E_o, or the angular frequency ω, would change the sign and magnitude of the flux of the protein. This would verify the existence of a binary filter point as well as give quantitative comparisons to theory. To this end preliminary single protein experiments were conducted using Bovine Hemoglobin (BHb) dissolved in a sodium acetate/acetic acid buffer of pH 4.5 and conductivity of approximately 325.0 $\frac{\mu S}{cm}$. Based on results from Douglas et. al. [16], the dimensional electrophoretic mobility of BHb was approximately $20.0e^{-5}\frac{cm^2}{Vsec}$. The syringe, which served as the inlet reservoir, was filled with approximately $15mL$ of protein solution, while the outlet reservoir contained approximately $40mL$ of the same solution. In all experiments, the concentration of the outlet reservoir was monitored with time.

Phase Dependence. The initial experiments were conducted using the larger separation cell. The choice of waveforms included $h(\omega t) = \sin(\omega t) - 0.05$ for the electric field $f(\omega t) = 2\cos(2\omega t)$ and $-2\cos(2\omega t)$ for the flow. The concentration in the outlet reservoir was found to decrease using the $-2\cos(2\omega t)$ mode and increase using $2\cos(2\omega t)$ mode. The results are shown in Figure (9). Note that a sign change of the flux resulting from a

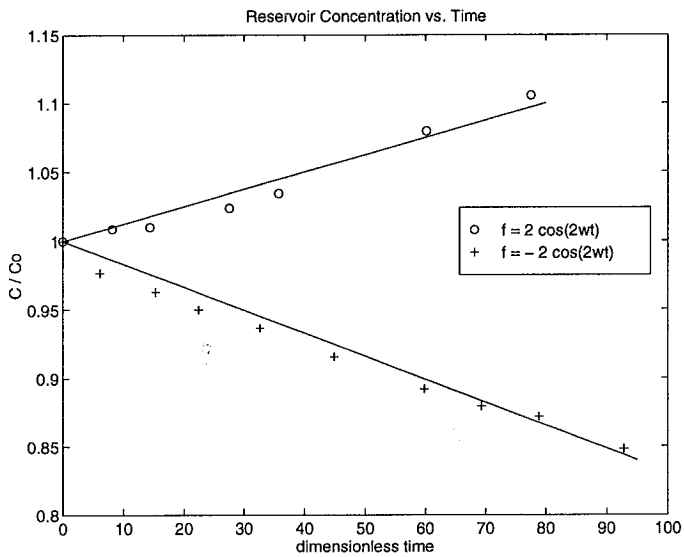

Figure 9: Reservoir Concentration vs. Time. Experimental Conditions: $\Delta x = 1.5cm$, $\omega = 0.068\frac{rad}{sec}$, $f(\omega t) = 2\cos(2\omega t), -2\cos(2\omega t)$, $E = E_o(\sin(2\pi\frac{t}{T}) - 0.05)$, $E_o = 19.6\frac{V}{cm}$, pH = 4.5, conductivity = $3.75e^{-4}\frac{S}{cm}$, $C_o = 2.2e^{-2}$ wt % BHb protein

180° phase change in the flow waveform agrees with theory. To test this phase dependence further, we examined the effect of a time dependent phase lag produced by the electric field waveform $h(\omega t) = \sin((2\pi - \frac{\pi}{15})t/T) - 0.05$, where T is the period of oscillation. The result of this experiment is given in Figure (10), where the dimensionless flux is plotted vs. phase angle. Again there is a qualitative agreement with theory.

Effect of the Mobility. Because of deficiencies in the larger cell mentioned above, the smaller cell was used in the subsequent experiments. Using this cell we examined the effect

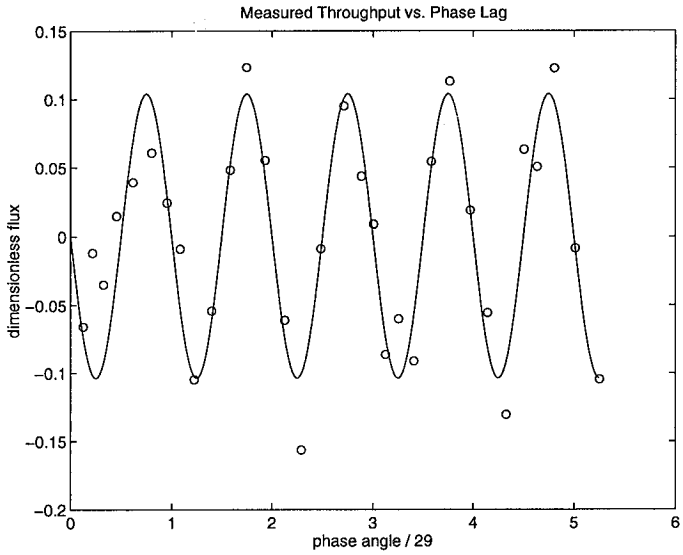

Figure 10: Measured Throughput vs. Phase Lag. Experimental Conditions: $\Delta x = 1.5cm$, $\omega = 0.068\frac{rad}{sec}$, $f(\omega t) = 2\cos(2\omega t)$, $E = E_o(\sin((2\pi - \frac{\pi}{15})\frac{t}{T}) - 0.05)$, $E_o = 25\frac{V}{cm}$, pH = 4.6, conductivity $= 3.25e^{-4}\frac{S}{cm}$, $C_o = 1.524e^{-2}$ wt % BHb protein

of varying α on the solute flux using the complex cross-flow waveform $f(\omega t) = 0.9\cos(\omega t) - 2\cos(2\omega t)$. The frequency was fixed at 0.136 $\frac{1}{sec}$ and the field strength varied from 5 to $25\frac{V}{cm}$. The results of our initial experiments are depicted in Figure (11).

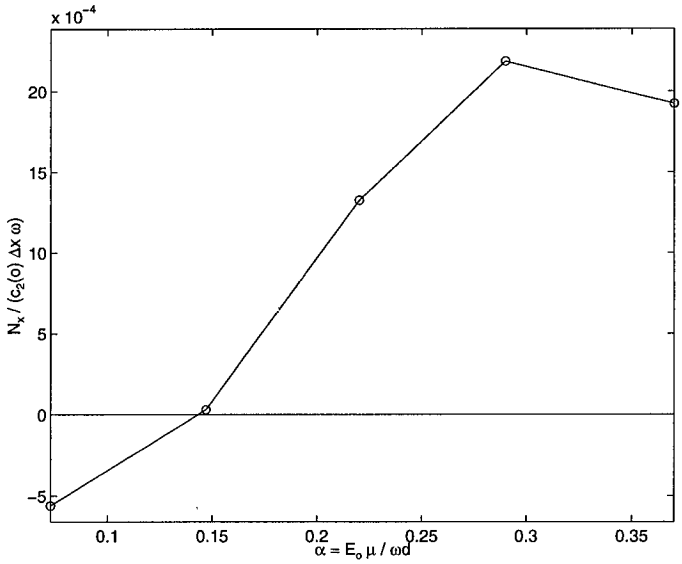

Figure 11: Measured Flux vs. α. Experimental Conditions: $\Delta x = 1.5cm$, $\omega = 0.136\frac{rad}{sec}$, $f(\omega t) = 0.9\cos(\omega t) - 2\cos(2\omega t)$, $E = E_o(\sin(2\pi\frac{t}{T}) - 0.05)$, $E_o = 5$ to $25\frac{V}{cm}$, pH = 4.5, $\sigma = 3.75e^{-4}\frac{S}{cm}$, $C_o = 2.2e^{-2}$ wt % BHb protein

Under these conditions it is seen that low values of the mobility led to a negative flux, while somewhat higher values led to a positive flux, yielding a binary separation. Although these results are in qualitative agreement with our theoretical model, the actual position of the critical mobility differs from that expected, and the magnitudes of the flux are far less than theory predicts. To investigate the source of these discrepancies, we examined the behavior of the individual crossflow modes.

To test the performance of the individual modes, our experiments used initially uniform concentrations and either $f(\omega t) = -\cos(\omega t)$ and $f(\omega t) = -\cos(2\omega t)$ for the flow waveform. The predicted flux in each case would be in the direction of the outlet reservoir, and would thus insure that the rise in reservoir concentration would be due only to the interaction of the two driving forces. For our experiments we chose $h(\omega t) = \sin(\omega t) - 0.05$ for the oscillation of the electric field, $\omega = 0.136$ for the frequency, $\Delta x = 4.0cm$ for the stroke length, E_o varying from $15 - 45V/cm$ for the electric field strength and reservoir volumes $V_1 = 15ml$ and $V_2 = 30ml$.

The results for $\cos(\omega t)$ and $\cos(2\omega t)$ are shown in Figures (12) and (13). For comparison,

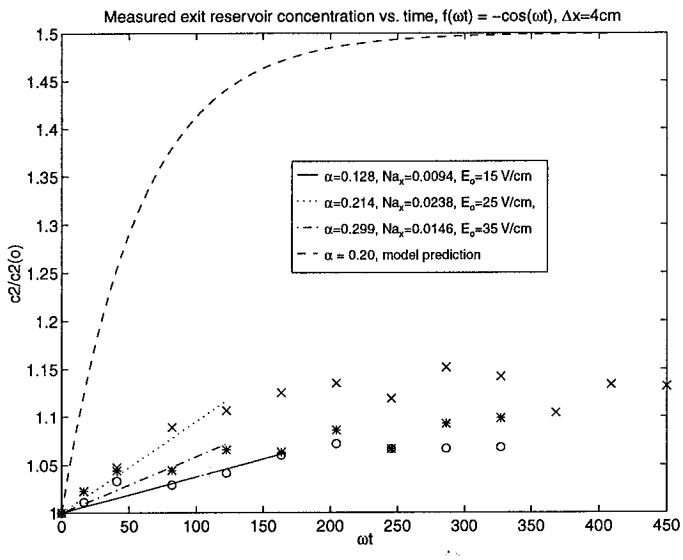

Figure 12: Reservoir Concentration vs. Time. Experimental Conditions: $\Delta x = 4.0cm$, $\omega = 0.136\frac{rad}{sec}$, $f(\omega t) = -\cos(\omega t)$, $E = E_o(\sin(2\pi\frac{t}{T}) - 0.05)$, $E_o = 15 - 35\frac{V}{cm}$, pH = 4.5, $\sigma = 2.75e^{-4}\frac{S}{cm}$, $C_o = 2.2e^{-2}$ wt % BHb protein

a numerically determined concentration profile (from equation (5)) has been included in both figures for an intermediate mobility. Note that the concentration begins to rise for all values of the α for both waveforms, and the relative flux increase with respect to the mobility agrees qualitatively with theory. However, after some time, the concentration in all $-\cos(\omega t)$ experiments begins to decrease and furthermore the magnitudes of the flux are far less than predicted. Conversely, Figure (12) shows that for the $-\cos(2\omega t)$ mode, the concentrations increase toward a steady value that is in good agreement with theory. Additionally, mass balance analysis following the experiment revealed a rise in concentration in the cell and a decrease in the syringe for the $-\cos(\omega t)$ experiments. The apparent focusing of solute in

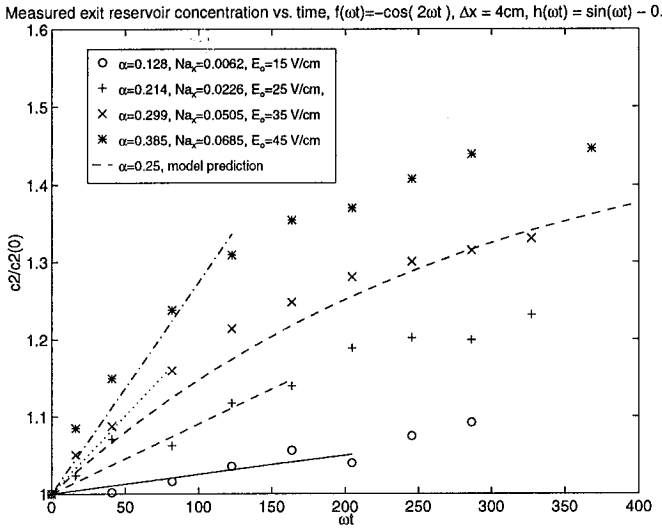

Figure 13: Reservoir Concentration vs. Time. Experimental Conditions: $\Delta x = 4.0cm$, $\omega = 0.136\frac{rad}{sec}$, $f(\omega t) = -\cos(2\omega t)$, $E = E_o(\sin(2\pi\frac{t}{T}) - 0.05)$, $E_o = 15 - 45\frac{V}{cm}$, pH = 4.5, $\sigma = 2.75e^{-4}\frac{S}{cm}$, $C_o = 2.2e^{-2}$ wt % BHb protein

the cell appeared to increase with increasing α. Furthermore, the effect was absent for the higher frequency mode.

Despite the discrepancies with theory, the approximate location of a separation point could be determined from the individual mode experiments. The results of one such experiment, using a binary protein mixture, is shown in Figure(14). Note that the concentration of Bovine Serum Albumen ($\alpha_{BSA} = 0.12$) increases with time while that of BHb ($\alpha_{BHb} = 0.32$) decreases, indicating a binary separation. Furthermore, the relative position of the critical mobility agrees with the experimental data of the individual modes, although not with the theoretical predictions.

Effect of the bias. Although these results were promising, the focusing effect observed in the $\cos(\omega t)$ experiments prevented the BOCE technique from being used for large scale continuous separations in its present status. This effect is evident in the results of Figure (14). Note that although the concentration of BHb protein decreases initially, the flux goes to zero after a short time. In an attempt to explain the source of the focusing phenomena, we consider the dependence of the induced migration on α for the oscillatory modes shown in Figure (2).

To begin we examine the $\cos(\omega t)$ mode (here the bias is 0), noting that maximum velocities are obtained when solute oscillates about one half of the channel ($\alpha = 0.25$). For $\alpha = 0.5$ however, solute will oscillate symmetrically with respect to the centerline of the channel, and in this case, no net migration is observed. Physically this is because at times when the solute reaches identical streamlines on each side of the centerline of the channel, the shearing effect of the bulk flow is equal in magnitude but opposite in sign. Therefore solute will always return to its beginning (x, y) position at the end of each period. Conversely, using the $\cos(2\omega t)$ mode, this symmetric steady state position optimizes the performance.

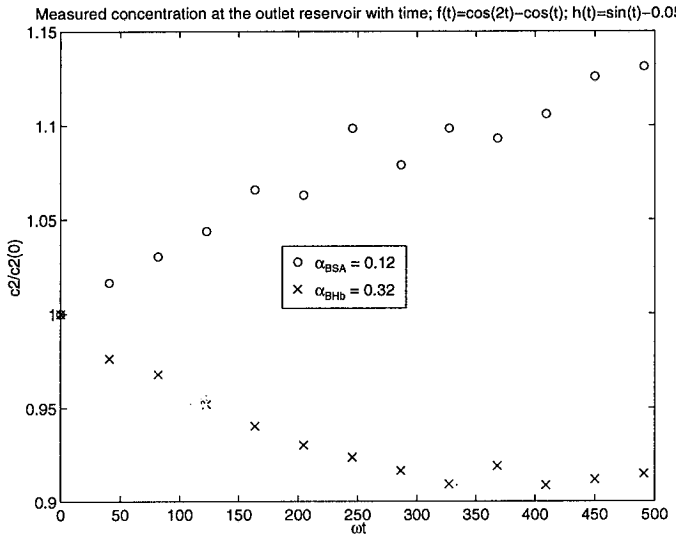

Figure 14: Reservoir Concentration vs. Time. Experimental Conditions: $\Delta x = 4.0cm$, $\omega = 0.136\frac{rad}{sec}$, $f(\omega t) = \cos(2\omega t) - \cos(\omega t)$, $E = E_o(\sin(2\pi\frac{t}{T}) - 0.05)$, $E_o = 25\frac{V}{cm}$, pH $= 4.5$, $\sigma = 2.75e^{-4}\frac{S}{cm}$, $C_{BHb}(0) = 1.0e^{-2}$ wt %, $C_{BSA}(0) = 2.0e^{-1}$ wt %

We can conclude that the steady state position about which an individual mode oscillates will have a large effect on the velocity induced for that mode.

The results of Figure (2), however are limited in that they do not consider the effects of diffusion. With diffusion present, the solute distribution will eventually oscillate about the centerline regardless of the value of the mobility for $\alpha \leq 0.5$, in the absence of a bias to the electric field. To study the competing effects of the bias and diffusion further, we ran numerical simulations for the individual modes for different values of δ. These results are shown in Figures (15) and (16) for the $\cos(\omega t)$ and $\cos(2\omega t)$ waveforms. For the $cos(\omega t)$ mode, the performance is optimized as the bias is increased, while the opposite is true for the higher frequency mode. From these results we predicted that δ may be used to move the steady state channel position of the solute distribution to improve the performance of an individual flow mode.

To test these predictions we repeated earlier experiments for the time dependent flow $f(\omega t) = -cos(\omega t)$ under similar conditions using higher electric field bias. The results of one such experiment are given in Figure (17) along with a concentration profile numerically determined from Equation (5). In agreement with predictions, the use of a higher bias resulted in a relative increase in the flux. This increase is attributed to the larger driving force toward steady state oscillations that are asymmetric with respect to the centerline of the channel. Although the observed flux has improved, the discrepancies between experiment and the flux predicted from equation (5) are significant.

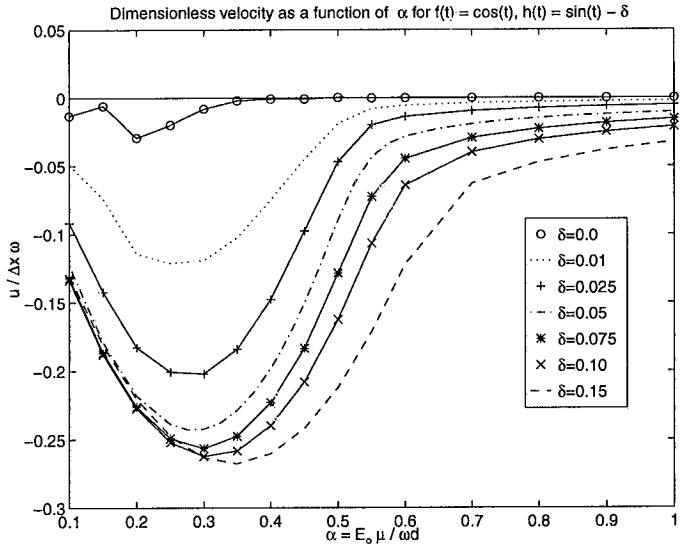

Figure 15: Plot of the dimensionless velocity vs. the dimensionless mobility for $\lambda = 5e^{-4}$, $f(\omega t) = \cos(\omega t)$, and $h(\omega t) = \sin(\omega t) - \delta$

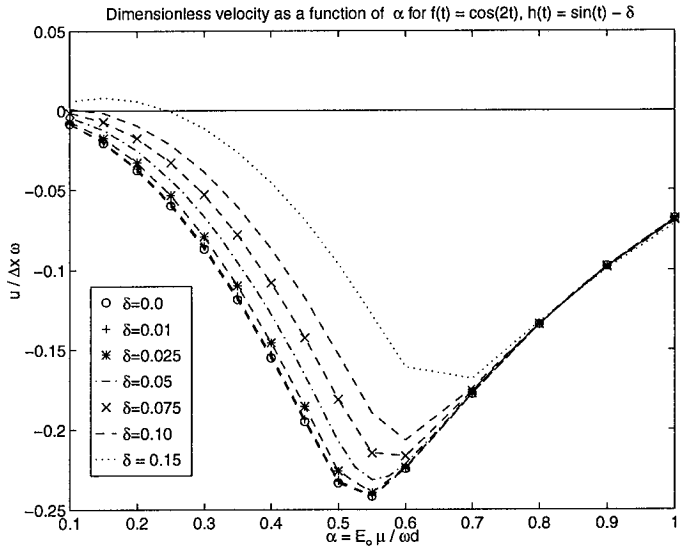

Figure 16: Plot of the dimensionless velocity vs. the dimensionless mobility for $\lambda = 5e^{-4}$, $f(\omega t) = \cos(2\omega t)$, and $h(\omega t) = \sin(\omega t) - \delta$

5 Numerical Results including Channel End Regions.

Although the numerical simulations for variable bias give important insight into the behavior of individual time dependent flow modes, experiments indicate that the effect of the bias alone is insufficient to explain of the discrepancies between experiments and the model predictions. To better understand the discrepancies, it is useful to consider the

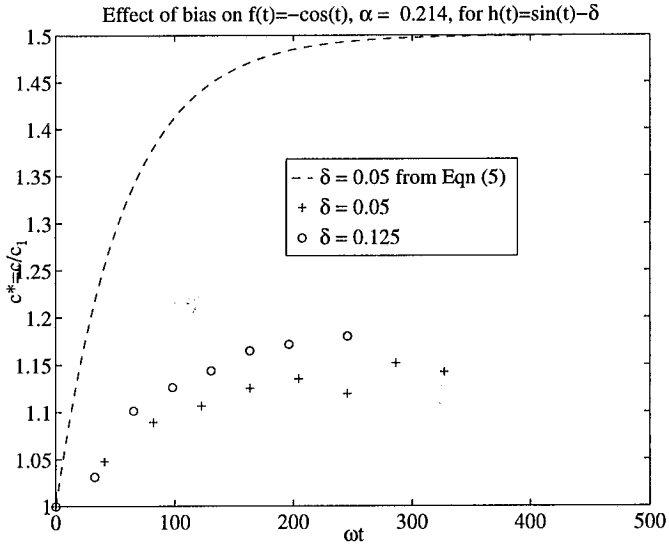

Figure 17: Reservoir Concentration vs. Time. Experimental Conditions: $\Delta x = 4.0cm$, $\omega = 0.136\frac{rad}{sec}$, $f(\omega t) = -\cos(\omega t)$, $E = 25(\sin(2\pi\frac{t}{T}) - \delta)\frac{V}{cm}$, pH $= 4.5$, $\sigma = 2.75e^{-4}\frac{S}{cm}$, $C_o = 2.0 - 2.2e^{-2}$ wt % BHb protein

characteristic time scales governing transport in the cell.

To begin we consider the motion of a solute species distributed about the center of the channel. The total (dimensionless) distance that the center of mass of this distribution travels across the channel gap width in any time period is equal to twice the dimensionless mobility α. Therefore the distance the distribution extends away from either channel wall is $1 - 2\alpha$. In the absence of any bias or diffusion, the use of a transverse oscillatory shear flow will (for any given α) either produce no net time averaged migration velocity for $f(\omega t) = cos(\omega t)$ or a maximum net velocity for a flow of twice this frequency, for reasons given previously. If diffusion is included, the steady state position about which the distribution oscillates will eventually move to the center of the channel, regardless of the initial position. If we include a small electric field bias, the position of the distribution will be forced toward one wall or another. The characteristic time to steady state can thus be expressed as $t_c = \frac{(1-2\alpha)}{(\alpha\delta+\lambda)}$. The key difficulty is that solute molecules are constantly entering and exiting the channel through the end regions. Because molecules enter the channel from a well mixed reservoir, they will enter at a uniform concentration irrespective of the electric field. The distribution will only reach its steady value (that for an infinite channel) after some time t_c has elapsed, which may be greater than the residence time of the solute in the channel.

To quantify the effects of the cell end regions, the earlier numerical code was revised to include not only the finite cell length but also the reservoir volumes and concentrations. The code made it possible to track the time history of the concentration profiles in the cell and reservoirs, thus simulating an actual experiment. For comparison, simulations parameters were chosen to match experimental conditions shown in Figures (12) and (13). The results of two such simulations, together with experimental results are shown in Figures (18) and (19).

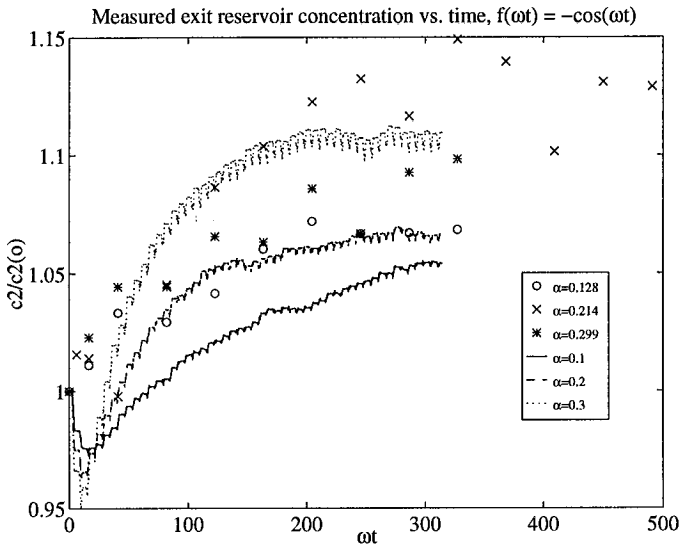

Figure 18: Reservoir Concentration vs. Time. Conditions: $\Delta x = 4.0cm$, $\omega = 0.136\frac{rad}{sec}$, $f(\omega t) = -\cos(\omega t)$, $E = E_o(\sin(2\pi\frac{t}{T}) - 0.05)$, $E_o = 15 - 35\frac{V}{cm}$, pH $= 4.5$, $\sigma = 2.75e^{-4}\frac{S}{cm}$, $C_o = 2.2e^{-2}$ wt % BHb protein

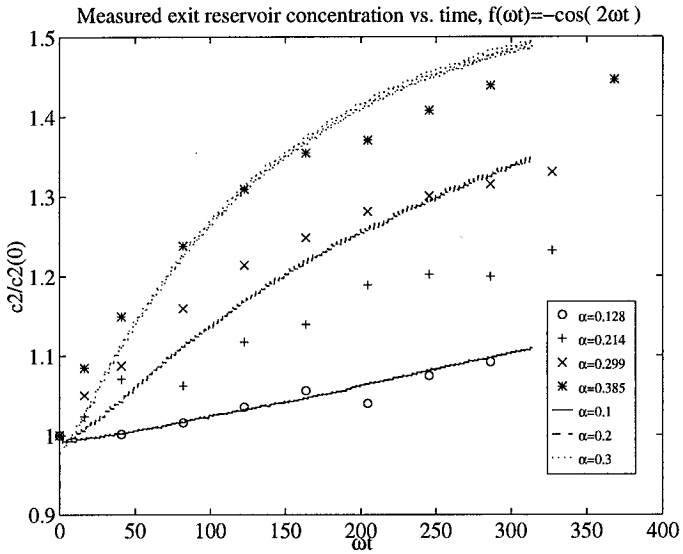

Figure 19: Reservoir Concentration vs. Time. Conditions: $\Delta x = 4.0cm$, $\omega = 0.136\frac{rad}{sec}$, $f(\omega t) = -\cos(2\omega t)$, $E = E_o(\sin(2\pi\frac{t}{T}) - 0.05)$, $E_o = 15 - 45\frac{V}{cm}$, pH $= 4.5$, $\sigma = 2.75e^{-4}\frac{S}{cm}$, $C_o = 2.2e^{-2}$ wt % BHb protein

In contrast to earlier models, this model which explicitly includes the entrance and exit effects does a good job of describing the observed fluxes for both oscillatory flow modes. Both simulation and experiment show that the $\cos(\omega t)$ fluid oscillation mode sucks in protein from

the reservoirs at both ends of the cell, raising the concentration in the cell far above that of the reservoirs and limiting the net rate of transport. In contrast the $\cos(2\omega t)$ mode does not appear to immobilize the protein to a significant degree and thus yields a flux and total transport that are much greater.

In order to produce a binary separation of protein species it is necessary to use a combination of at least two Fourier modes of the fluid flow. Because of end effects, the $\cos(\omega t)$ mode is not suitable for BOCE operation. Thus a binary separation must be achieved using a combination of the $\cos(2\omega t)$ mode and a small amplitude steady flow. Numerical simulations and preliminary experiments have indicated that this is a promising approach free of significant end effects. We are currently investigating this approach further.

6 Conclusions

In this report we have described a novel electrophoretic separation technique, Binary Oscillatory Crossflow Electrophoresis. By imposing an oscillatory electric field across the narrow gap of a thin rectangular channel, solute molecules will undergo periodic motion with amplitude depending on the dimensionless electrophoretic mobility α. With the addition of a transverse oscillatory shear flow, solute species can be made to migrate in either direction in response to a change of phase of the oscillatory flow, even in the absence of initial concentration gradients. For correct choice of operating parameters, the technique can be used to separate charge species based on differences in α. We have presented a model that predicts the oscillatory behavior of charged species and allows estimation of both the magnitude of the induced convective velocity as well as the effective enhancement to the diffusivity as a function of α. Additionally, our model accounts for both finite cell lengths and reservoir volumes and predicts the time history of the concentration profile throughout the system. These latter predictions have been quantitatively supported through experiments using single protein species.

In its present form, the BOCE technique is incapable of sustaining a binary separation using a combination of purely oscillatory shear flows $f(\omega t) = \cos(\omega t)$ and $\cos(2\omega t)$ in finite channels. This has been attributed to fluid oscillations into and out of the active electric field regions at the ends of the cell. For time dependent flows of the same frequency of the applied electric field oscillations, any initially induced flux will eventually vanish. However, the technique holds great promise for use with more complex flows. For example, we have recently modelled the effect of adding a small steady flow component to the time dependent flow mode $\cos(2\omega t)$. Preliminary numerical and experimental results suggest that this combination is unaffected by cell end effects and will sustain continuous binary separations. This topic will be the focus of future research.

References

[1] Tisilius, A., "A New Apparatus for Electrophoretic Analysis of Colloidal Mixtures," Trans. Farad. Soc.,**33**, 524 (1937)

[2] Saville, D. A., and W. B. Russell, "Colloidal Dispersions," Cambridge University Press, New York, 1989

[3] Caldwell, K.D., L.F. Kesner, M.N. Myers and J.C. Giddings, "Electrical Field Flow Fractionation of Proteins," Science, **Vol 21**, 269 (1972)

[4] Ivory, C.F., "The Prospects for Large-Scale Electrophoresis," Separation Science and Technology, **23**, (8 & 9), 525, (1988)

[5] Rhodes, P.H., R.S. Snyder, and G.O. Roberts, "Electrohydrodynamic Distortion of Sample Streams in Continuous Flow Electrophoresis" J. Colloid and Interface Sci. **Vol 129 No 1**, 78 (1988)

[6] Saville, D.A., "Electrohydrodynamic Deformation of a Particulate Stream by a Transverse Electric Field " The American Physical Soc. **Vol 71 No 18**, Nov 1, 2907 (1993)

[7] Giddings, J.C., M.N. Myers, K.D. Caldwell, and S.R. Fisher, "Analysis of Biological Macromolecules and Particles by Field-Flow Fractionation" Methods of Biochemical Analysis, **Vol 26** 79 (1976)

[8] Philpot, J.St.L.,"Apparatus for Continuous-Flow Preparative Electrophoresis," Methodological Developments in Biochemistry: 2 Preparative Techniques, E. Reid, ed., Longmanss, England, 81, (1973)

[9] Davis, J.M., F.-R. Fan, and A.J. Bard, "Retention by Electrical Flow Fractionation of Anions in a New Apparatus with Annular Porous Glass Channels," Analytical Chemistry. bf 1987, 59, 1339-1348

[10] Thormann, W., M.A. Firestone, M.L. Dietz, T. Cecconie, and R.A Mosher, "Focusing Counterparts of Electrical Field Flow Fractionation and Capillary Zone Electrophoresis," Journal of Chromatography, **461**, 95, (1989)

[11] Giddings, J.C., "Cyclical Field Flow Fractionation: A New Mwthod Based on Transport Rates," Analytical Chemistry, **Vol 58**, 2052, (1986)

[12] Shmidt, J.L., and H.Y. Cheh, "Continuous Free-Flow Fractionation in an vAlternating Field with a Variable Buffer Flow," Separation Science and Technology, **25** (7 & 8), 889, (1990)

[13] Chandhok, A.K., and D.T. Leighton, Jr.,"Oscillatory Cross-Flow Electrophoresis," AIChE Journal, **Vol 37 No 10**, 1537 (1991)

[14] Aris, R., "On the Dispersion of a Solute by Diffusion Convection and Exchange Between Phases,"Proc. Roy. Soc. A, **252**, 539 (1959)

[15] Watson, E.J., "Diffusion in Oscillatory Pipe Flow," Journal of Fluid Mechanics, **Vol 133**, 233 (1983)

[16] Douglas, N.G., A.A Humffray, H.R.C. Pratt,and G.W. Stevens,"Electrophoretic Mobilities of Proteins and Protein Mixtures," Chem Eng Sci, **Vol 50 No 5**, 743 (1995)

8 Students supported under this grant

There were two graduate students supported under NASA grant NAG-8-1080.S over the award period 8/94 - 2/97:

1)Richard Molloy, Ph.D. exp. (1998), "Binary Oscillatory Crossflow Electrophoresis"

2)Yolanda Van Lishout, Ph.D. (1997), "Oscillatory Membrane Separations"

A portion of the latter thesis work dealt with dispersion produced from oscillatory flows in parallel channels. This research provided valuable insight into dispersion observed in the BOCE cell and suggested possible geometries for scaleup of an electrophoretic device.

9 Publications resulting from this grant

1)Molloy, Richard F., Christopher T. Gallagher, and David T. Leighton, Jr., "Binary Oscillatory Crossflow Electrophoresis," NASA Conference Publication. n 3338 1996. NASA, Cleveland, OH, USA p 723-728

2)In addition, two manuscripts detailing work supported in part by this grant are being prepared for publication.

3)The results of this work will be presented at the annual AIChE conference in Los Angeles, CA in 11/97.